Expert Systems with Applications 38 (2011) 10822–10830

Contents lists available at ScienceDirect

Expert Systems with Applications

journal homepage: www.elsevier.com/locate/eswa

Rotor fault diagnosis system based on sGA-based individual neural networks

Chin-Sheng Chen *, Jian-Shiu Chen

Graduate Institute of Automation Technology, National Taipei University of Technology, 1, Sec. 3, Chung-Hsiao E. Rd., Taipei 106, Taiwan, ROC

ARTICLE INFO

Keywords:
Fault diagnosis
Order tracking
Spectrum analysis
Structure genetic algorithm
Neural network

ABSTRACT

This paper proposes a robust fault diagnosis system of rotating machine adapting machine learning technology. The kernel of this diagnosis system includes a set of individual neural networks based on structured genetic algorithm (sGAINNs). First, the frequency characteristics from differential signals, including fast Fourier transform (FFT) and full spectrum, are used to feed into the sGAINNs corresponding to assigned faults to emphasize the phenomenon of each fault. Especially, the structured genetic algorithm is applied to get the optimal parameters of the above sGAINNs. In the final step of proposed diagnosis system, the evaluated indexes from sGAINNs are synthesized by a reasoning engine to identify the faults in the rotor system. Finally, six common faults of rotor system, unbalance, bow, misalignment, rub, whirl, and whip, are generated from a rotor kit, produced by Bently Nevada Corporation, to verify the performance of this diagnosis system. The advantage of this diagnosis system is that the optimal sGAINNs parameters can be automatically obtained, the local optimal solutions can be reduced and the diagnosis accuracy can be improved.

1. Introduction

Condition monitoring and fault diagnosis play crucial roles in avoiding serious damages in a rotating machinery system. Traditionally, regular maintenance of a rotor system is needed to prevent the sudden functionless in most industries. However, the off-line regular maintenance must shut down the rotating machinery that will waste the operation resource. And the seriousness and type of equipment fault must be precisely identified with dismantling a machine, yet the very act of dismantling can impose negative impacts on the machine's performance. Fault diagnosis system has accordingly been developed to avoid unnecessary waste of time, effort, money and other resources.

A fault diagnosis system (Diao & Passino, 2004; Stephan & Zhongxiao, 2008) works to both monitor and diagnose. At present, there are many techniques acoustic emission (Toutountzakis, Tan, & Mba, 2005), vibration signal (Donald & Charles, 2003; Gebraeel, Lawley, Liu, & Parmeshwaran, 2004) and oil analysis. Vibration signal, a well established and easy-to-use approach, remains the most common among all monitoring techniques. The spectrum data can be clearly classified between the different of normal and abnormal status. Hence, its magnitude is suitable to be used for the detection of the fault.

Full spectrum plot (Goldman & Muszynska, 1999; Laws, 1998; Southwick, 1993, 1994) was introduced by Bently Nevada Corporation in 1993 as an improvement on its "traditional spectrum". The spectrum helps to extract and display significant information from the vibration signal.

There are many diagnosis algorithms available, notably neural networks, genetic neural network and fuzzy neural network. These algorithms based on a series of standard fault symptoms to identify the fault in the system. The neural network was always trained by collecting the spectrum of vibrations obtained from the operating machine in fault diagnosis system (Hayashi, Asakura, & Zhang, 2002; Wu & Liu, 2009). However, the unconstrained neural network parameters will yield long trained epoch. The genetic neural network (Fu, Chen, Yu, & Zeng, 2006) carries on the compounded training with neural network; furthermore using genetic algorithm to optimize neural network parameters. The fuzzy neural networks (Zhang, Asakura, Xu, & Xu, 2003) are trained to memorize standard patterns, and it can make diagnosis by association.

This paper mainly describes fault diagnosis system includes two stages: (1) pre-processing of vibration signal, (2) fault diagnosis. The architecture of this rotor diagnosis system is shown in Fig. 1. In first stage, the raw data "signal" are acquired from a rotor data acquisition system. Through using order tracking technique let the signals transform into useful frequency information by FFT and full spectrum. The plane information of orthogonal transducers is used to represent the vibration signal because the full spectrum is more robust than traditional half spectrum. Then, Data 1 and Data 2 are corresponds to FFT and full spectrum are respectively fed into two kinds of sGAINNs corresponding to the above two characters for all faults.

In second stage, the training phase is processed before diagnosis phase. This diagnosis system is constructed with a set of sGAINNs,

* Corresponding author. Address: Graduate Institute of Automation Technology, National Taipei University of Technology, NTUT Box 4325, 1, Sec. 3, Chung-Hsiao E. Rd., Taipei 106, Taiwan, ROC. Tel.: +886 2 27712171x4325; fax: +886 2 87733217.
E-mail address: saint@ntut.edu.tw (C.-S. Chen).

0957-4174/$ - see front matter © 2011 Elsevier Ltd. All rights reserved.
doi:10.1016/j.eswa.2011.02.074

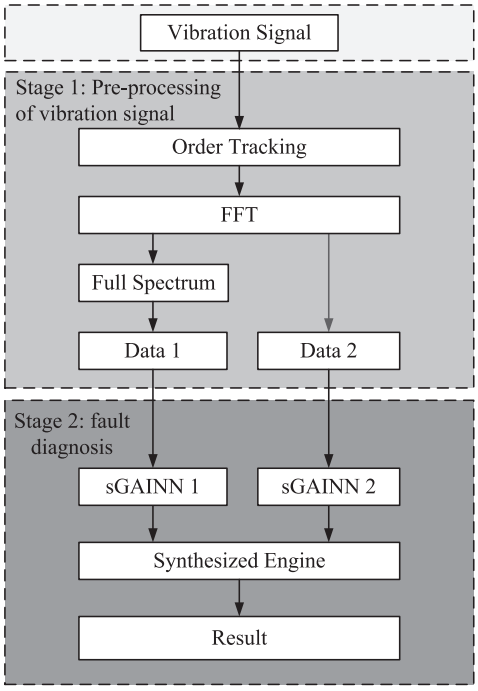

Fig. 1. The architecture of rotor diagnosis system.

each network corresponds to a set of assigned signal characteristic such as sGAINN1 and sGAINN2. And the evaluated indexes from each sGAINN are synthesized by a reasoning engine. Furthermore, the structure genetic algorithm (sGA) is applied to optimum the parameters of neural network in order to improve the trained robustness and enhance the diagnose accuracy of this diagnosis system.

2. Rotor system and data acquisition

2.1. Hardware setup

In this paper, the hardware of experimental rotor system is produced by Bently Nevada Corporation. It is applied to simulate the assigned faults of rotating machine to train and test the performance of proposed diagnosis system. Two bearings and two orthogonal pairs of transducers are setup to support the shaft and acquire the vibration signals from two planes in the rotor system respectively, as shown in Fig. 2.

Then, the orbit combine timebase plot of vibration signal *Y* axis with *X* axis to provide plane information of vibration signal when rotor is running, which is shown in Fig. 3. For each orbit, the keyphasor incurs in black dots to indicate the start point of orbit pose. Furthermore, the location of keyphasor and orbit can be used to calculate the full spectrum.

2.2. The common fault of rotor system

This paper chooses six common faults of rotor system such as unbalance, misalignment, bow, rub, whirl and whip. The plane information is transformed into spectrum information by FFT and full spectrum. The spectrum information cannot only reduce data complexity but also retain more vibration information. Table 1 shows the characteristics of these common faults with two type analysis methods. The following characteristics to each common fault are sufficiently discussed with Taiwan Power Research Institute.

2.3. Enhanced fixed sample-rate order tracking (EFSROT)

In fixed sample-rate order tracking (FSROT) (Bai, Jeng, & Chen, 2002; Fyfe & Munck, 1997), the distance between two adjacent sampling frequencies of the spectrum can be either enlarged or reduced but needs to remain fixed. FSROT is capable of changing

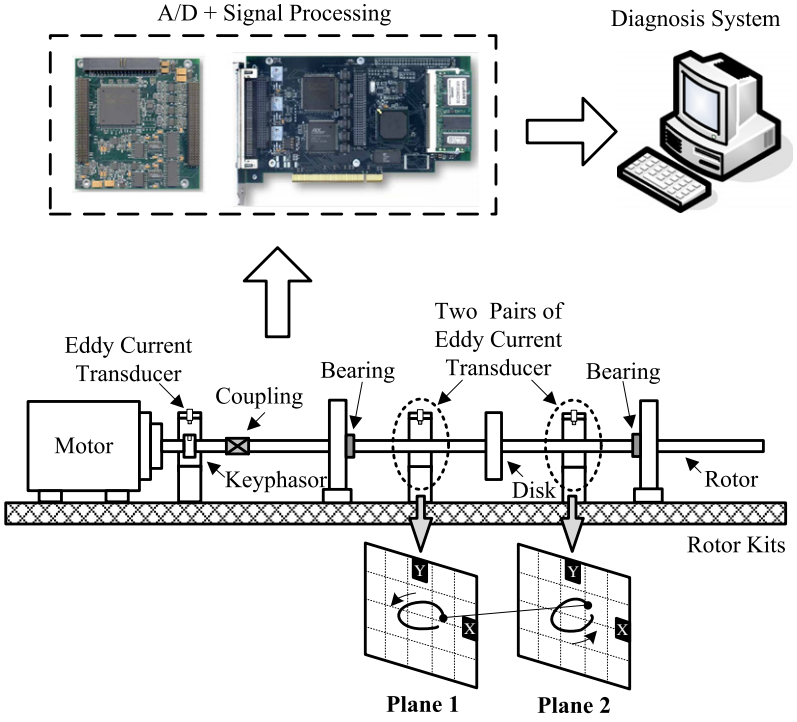

Fig. 2. The hardware setup of rotor diagnosis system.

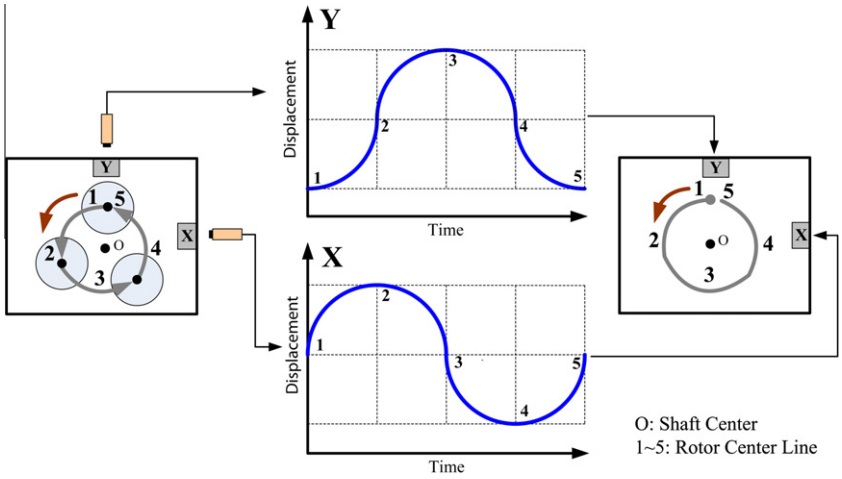

Fig. 3. Plane information of vibration signal.

Table 1
Rotating machinery malfunctions and its characteristics.

Faults	Analysis method	Characteristic
Unbalance	FFT	♦ Amplitude of 1*X* is larger than the other harmonic frequency
	Full spectrum	♦ Amplitude of 1*X* is larger in forward and backward direction
Misalignment	FFT	♦ Amplitude of 2*X* is larger; therefore the harmonic frequencies have less amplitude in 1*X* and 3*X*
	Full spectrum	♦ Amplitude of 2*X* is much larger in forward and backward direction, the other harmonic frequencies with less amplitude in 1*X*, 3*X*, and 4*X*
Bow	FFT	♦ Amplitude of 1*X* is larger; therefore the harmonic frequencies have less amplitude in 2*X* and 3*X*, respectively
	Full spectrum	♦ Amplitude of 1*X* is much larger in forward and backward direction, the other harmonic frequencies with less amplitude in 2*X* and 3*X*, respectively
Rub	FFT	♦ Amplitude changes with rotor speed. Besides dominant frequency with some amplitude, the other harmonic and subharmonic frequencies also have less amplitude
	Full spectrum	♦ Amplitude of 1*X* in forward and backward direction has larger value; the other harmonic and subharmonic frequencies also have less amplitude in forward and backward direction
Whirl	FFT	♦ Amplitude occurs near 0.42*X*–0.48*X*
	Full spectrum	♦ Amplitude occurs near 0.42*X*–0.48*X* just in forward direction
Whip	FFT	♦ Amplitude occurs near 0.5*X*
	Full spectrum	♦ Amplitude occurs near 0.5*X* in both forward and backward direction

the location of spectrum resolution, tracking running frequencies and reducing leak of energy. FSROT, however, is less powerful in terms of running speed; it is thus usually applied to large-scale machines with slack acceleration. This paper proposed a enhance technique to increase FSROT ability for varying shaft speeds, non-stationery signal, and uncertainty from measurement. The architecture of this order tracking technique is shows as Fig. 4. Thus, the fundamental of EFSROT is to adjust the sampling length of every acquisition by A/D so the purpose of tracking speed can be achieved. The main steps of EFSROT can be classified as follows:

2.3.1. Optimal fundamental frequency

This paper hopes to obtain the spectrum amplitude located at the actual vibration frequency; adjusting the sampling length in line with the actual vibration frequency is therefore needed. Thus, this paper adopted signal to noise ratio (S/N) to find the optimum fundamental frequency which is most close to the actual vibration frequency. The S/N measures variability around target performance. The higher S/N value indicates the more precise fundamental frequency is found. S/N can be written as

$$S/N = -10\log\frac{\sum_{i=1}^{n}(y_i - m)^2}{n} \quad (1)$$

where y_i $(1 \leqslant i \leqslant n)$ is rotor shaft speed per revolution, m is reference speed, and n is numbers of keyphasor interval.

For comparisons, different S/N values are calculated by two reference speeds (m): one is rotor speed at first period (f_{first}), and the other one is the average rotating speed per second ($f_{average}$). Then, the system refers to the calculation result to determinate the better one as optimal fundamental frequency (1*X*). Furthermore, this system uses down sampling technique to reduce the number of 10 k sampling points which based on 10 kHz sampling rate to determined the lowest frequency. For example, a rotating signal is measured shows as Table 2. The determinate fundamental frequency is located at 2.57 Hz which mismatch between the sampling frequency and the actual frequency as well as leak of energy can be avoid, because the sampling points are reduced to 3892 (10000/2.57 + 1 = 3892) points. Fig. 5 shows the tracking results in the cases of adjusted and unadjusted sampling lengths. Thus, the optimal frequency and the lowest resolution have been determined.

2.3.2. Increasing frequency resolution

Though the first step obtains precise multiple frequency of vibration frequency, which will induce the side effect of low resolution. Thus, interpolation needs to be adopted to increase frequency resolution. While resolution should as large as possible, it

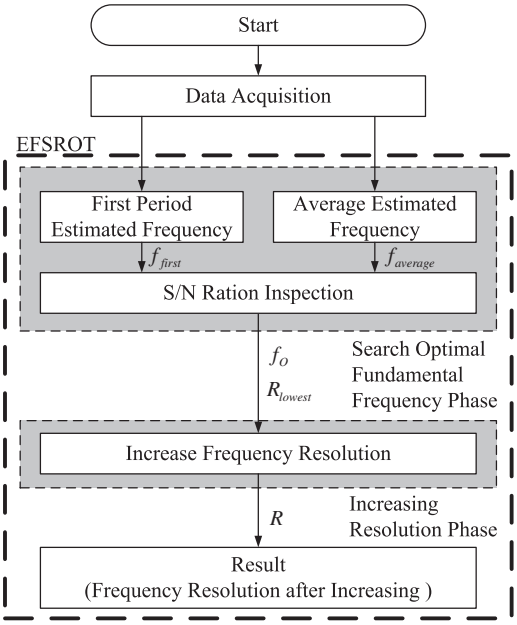

Fig. 4. The architecture of EFSROT. Here f_{first} is rotor speed at first period, $f_{average}$ is the average rotating speed per second, f_O is optimal fundamental frequency, R_{lowest} is lowest numbers of resolution, and R is numbers of resolution after adjusting.

Table 2
The estimated fundamental frequency.

Item	Calculated frequency (Hz)	*S*/*N* ratio
First period frequency	2.57	−3.0
Average frequency	2.56	−6.0

cannot exceed the maximum sampling resolution. As the previous step, the optimal vibration frequency is set at 2.57 Hz, and the maximum sampling resolution is 10,000 points. Then, the number of sampling point us adjusted to 7783 (10000/2.57 × 2 + 1 = 7783) points. The results after increasing frequency resolution are shown in Fig. 6.

3. Pre-processing of vibration signal

This paper gets the signals from an orthogonal pair of vibration transducers in the rotor system. The signal is transformed into useful frequency information by FFT and full spectrum. The data acquiring frequency characteristics from these information are Data 1 and Data 2. They can emphasize the phenomenon of each fault, and then help sGAINNs to learn the parameters of each network. Fig. 7 shows the pre-processing scheme of vibration signal.

3.1. The frequency of vibration signal

Rotor shaft in rotating can generate the vibration frequency which is the composition of many different frequencies. The frequency of vibration signal can help to make an accurate rotor diagnosis; it sometimes appears as a series of harmonics. The lowest frequency in the series is almost called the fundamental frequency, and a number of frequencies are at integer multiples of the fundamental frequency. Often, the fundamental is 1*X*, corresponding rotating speed of rotor, but it can also be any frequency such as 1/2*X*, 3/2*X*, 2*X* and 3*X*.

3.2. FFT and full spectrum transformation

When frequency information is used to evaluate machine condition, the most powerful plot for this purpose is the spectrum plot. The spectrum plot is created from the signal of a single transducer,

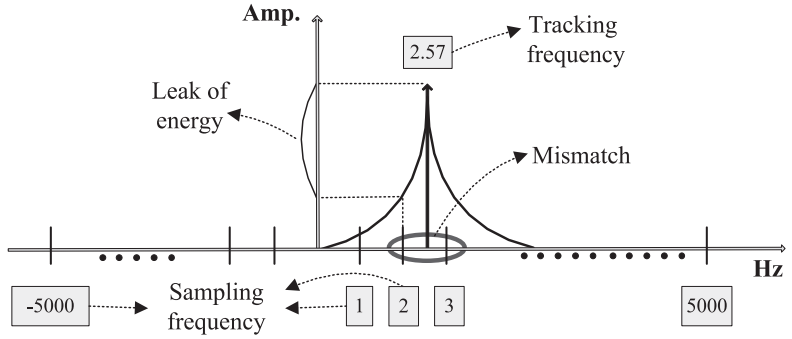

(a) The sampling frequency does not match tracking frequency.

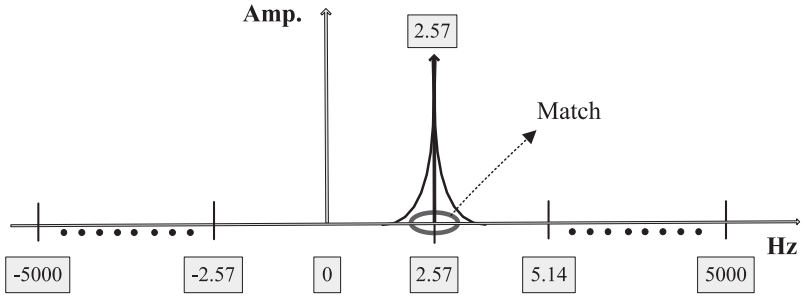

(b) The sampling frequency matches actual frequency after adjusting.

Fig. 5. Adjusting the sampling length.

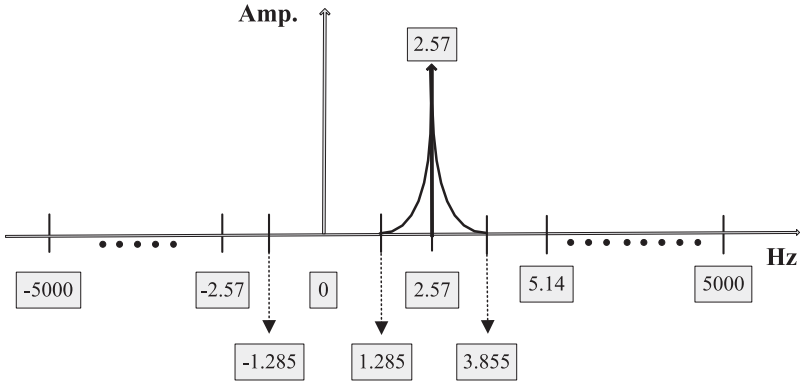

Fig. 6. Adding frequency resolution.

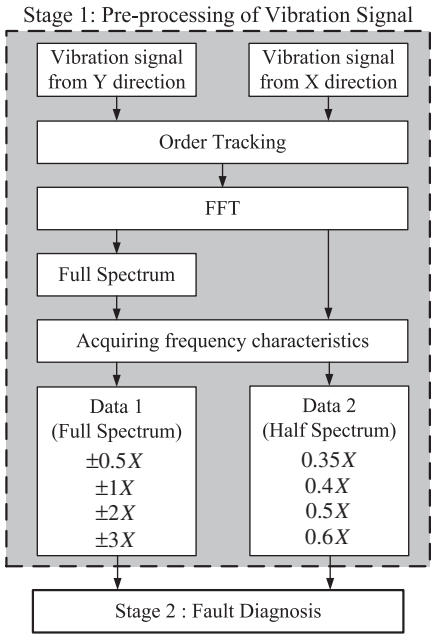

Fig. 7. The pre-processing scheme of vibration signal.

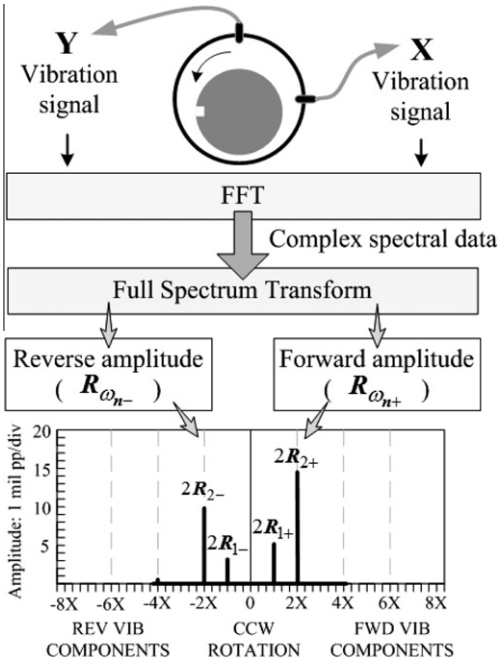

Fig. 8. Obtaining a full spectrum (from orbit magazine).

its objective is to extract and display significant diagnostic information. We refer to this conventional spectrum plot as the half spectrum plot. An important new tool, the full spectrum plot, has been developed in the past few years. It uses the signals from an orthogonal pair of vibration transducers. The full spectrum plot contains much information than the half spectrum plot, including vibration precession direction and orbit ellipticity. It is so important for machinery diagnostics. Fig. 8 shows the full spectrum that is calculated by performing an FFT on each transducer waveform.

In the full spectrum, training data is collected from pairs of amplitude of primary frequencies, which can present information about the magnitude and phase of every filter orbits.

One process can understand the correlation between the orbit and full spectrum by the filtered orbit. An expansion divides the direct orbit into a series of filtered orbit (Fig. 9). Each filtered orbits is elliptical shape and can be presented as sum of two circular orbits: one is forward, and one is reverse. Therefore, vector $\vec{r}$ of elliptical orbit is a sum of vector of the instantaneous position on the forward and reverse orbits:

$$\vec{r} = R_{\omega+} \cdot e^{j(\omega t+\alpha_\omega)} + R_{\omega-} \cdot e^{j(\omega t+\beta_\omega)}. \quad (2)$$

Here $R_{\omega+}$ and $R_{\omega-}$ are the radiuses of the forward and reverse orbit, ω is the frequency of filtering, and α_ω and β_ω are phases of forward and reverse response. The major axis of the filtered elliptical orbit is $R_{\omega+} + R_{\omega-}$ and its minor axis is $|R_{\omega+} - R_{\omega-}|$. The angle between the horizontal probe and the ellipse major axis is $(\beta_\omega - \alpha_\omega)/2$. Fig. 10 shows 1*X* filtered orbit and more information between orbit and full spectrum.

4. Fault diagnosis

After the vibration signal pre-processing stage, the spectrum information are fed into stage two to perform the fault diagnosis, which is shown in Fig. 11. Data 1 and Data 2 are full spectrum and half spectrum respectively. Half spectrum NN use 0.35*X*, 0.4*X*, 0.45*X* and 0.5*X* amplitudes as half spectrum characteristics; full spectrum NN use ±0.5*X*, ±1*X*, ±2*X* and ±3*X* amplitudes represent the full spectrum characteristics. These information are respectively fed into two kinds of INNs. Finally, two kinds of result stages are synthesized to evaluate diagnosis result.

4.1. INN diagnosis system

Neural networks (NNs) have been widely researched and applied in diagnosis system for some years. It is applied to model a real world system by tuning a set of weights, which are used to

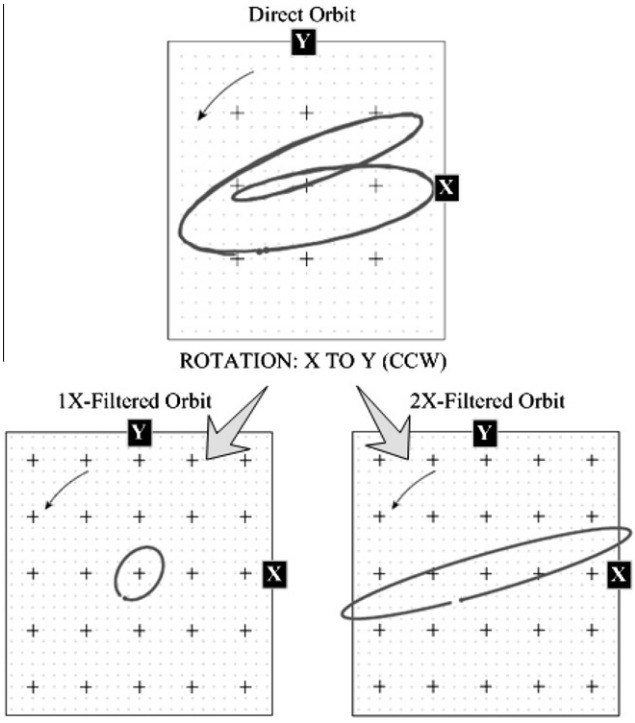

Fig. 9. Direct orbit transforms into filtered orbit (from orbit magazine).

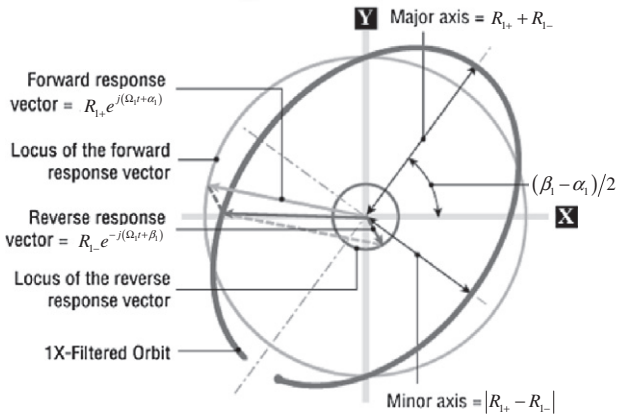

Fig. 10. 1X orbit enlarged to show detail (from orbit magazine).

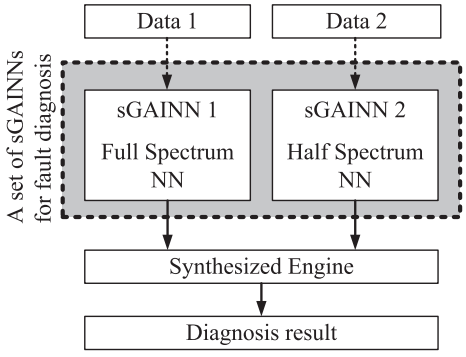

Fig. 11. Fault diagnosis process.

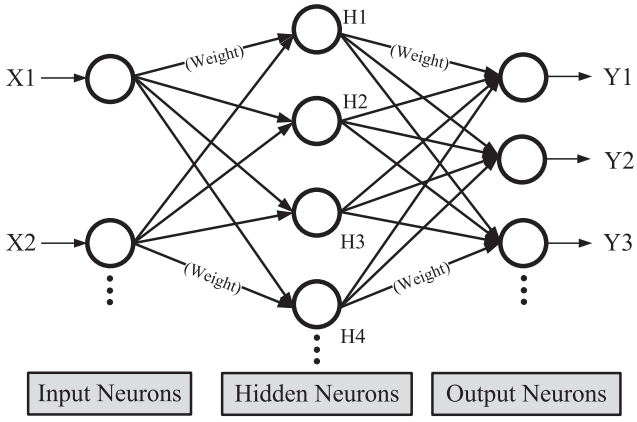

Fig. 12. The connections of every neuron in the network.

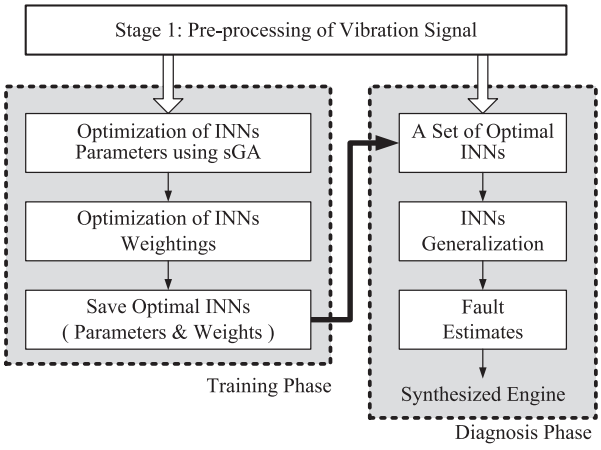

Fig. 13. INNs diagnosis system.

learn the relationship between given inputs and appropriate outputs. These weights are associated with the connections of every neuron in the network (Fig. 12). The NN weights adjust automatically in the training phase by minimizing the error between the output from the network and the desired output.

As mentioned above, each INN will learn the optimum parameters, and then diagnose each signal characteristic. Fig. 13 shows the flow chart of INNs constructing process. When INNs start to learn, training data and INN parameters must be determined firstly. The INN parameters include number of training times, number of neuron of hidden layer, learning rate, and momentum factor. Therefore, the above acquiring signal characteristics are applied as training data and the optimal parameters are obtained using structured genetic algorithm (sGA) method (Dasgupta & Mcgregor, 1992). When optimal INNs were found, INNs parameters and weights were saved and the training phase of INNs was finished.

After the training phase, the diagnosis phase is applied to obtain the fault estimates form each INN. Because this paper had two kinds of training data, it also had two kinds of INNs. When giving the frequency characteristics of unknown vibration signals to a set of INNs, it could get two kinds of estimates. The results will feed into synthesized reasoning engine to identify the most possible faults.

4.2. Optimization of INNs

4.2.1. INN parameters optimization using sGA

The advantage of NNs is its ability to learn and generalize from data. After training, NNs can produce appropriate outputs from

input of unknown class. It is useful to obtain classification applications. But, it has the disadvantage of limited theoretical background in identifying the optimal architecture of NN parameters, such as number of neurons, number of hidden layers, learning rate and training times. The NNs' parameters are commonly set by trial and error, which is time-consuming. This method is sometimes unable to obtain the best NN performance.

An optimal searching algorithms based on the mechanics of natural selection and genetics as observed in the biological world called Genetic algorithms (GA). GA is done by the global searching in the solving space with the processes of random and evaluation not limited and existed by the continuity or the derivatives can be regarded as one robust searching algorithm.

In traditional GA, after initial generations, improvement becomes slow as the genetic diversity of the initial population is diminished through the process of natural selection. One such model is called structured genetic algorithm (sGA), which capable of providing simple genetic approaches in its redundant genetic material and a gene activation mechanism. In this paper, the architecture of optimal NN parameters searching scheme is shown in Fig. 14. In the initial population step, a gene structure hierarchically categorizes genes into different groups, which are referred to NN parameters: *training generation*, *neuron numbers of hidden layer*, *learn speed* and *momentum factor*. These parameters are encoded as sets of genes by real number coding. Genes that are located in control level acts as switches, which control the activation state of genes located at lower gene levels. When genes are deactivated these genes still exist in the genotype and are capable of being propagated to future generations, however, the traits encoded by these genes do not get expressed in the phenotype.

The sGA achieves this evolution by repeatedly applying three genetic operators to the chromosomes in the population: crossover, mutation and structure activation respectively. In this paper,

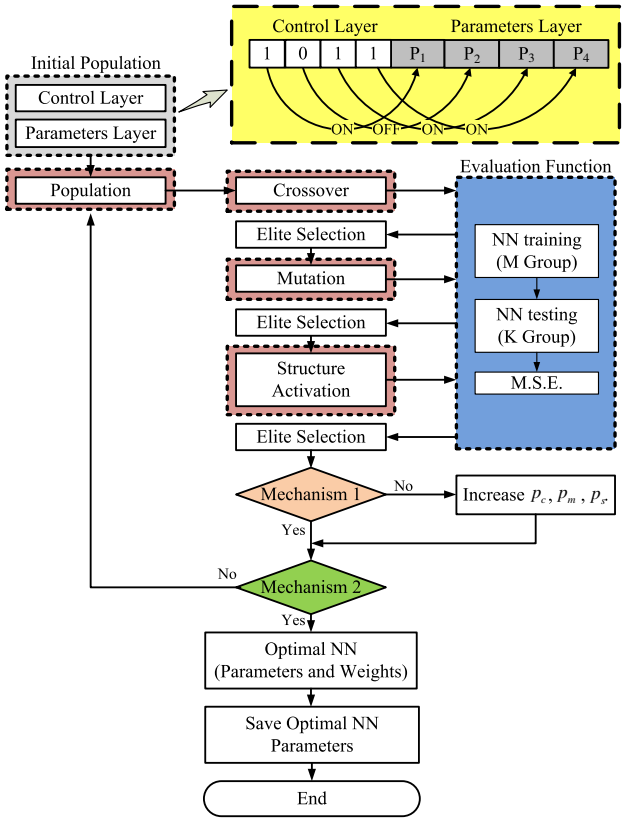

Fig. 14. The architecture of sGANN.

crossover executes through two ways to generate new individuals in the current gene pool, one is two randomly selected individuals by swapping portion of individuals; the other one is obtained by an alternative expression as (3) to generate new individuals.

$$\begin{aligned} V_1' &= \lambda V_1 + (1-\lambda)V_2 \\ V_2' &= \lambda V_2 + (1-\lambda)V_1 \end{aligned} \tag{3}$$

where V_1' and V_2' are child individuals; V_1 and V_2 are genes of parent individuals; λ is random number in the range [0, 1].

Mutation executed by an expression (4) base on the pre-determined upper limit and lower limit of the four INN factors to evolve new individuals.

$$\begin{aligned} &V_n' = V_n + \Delta(V_n^U - V_n) \\ &\text{or} \\ &V_n' = V_n - \Delta(V_n - V_n^L) \end{aligned} \tag{4}$$

where V_n' is the child individuals; V_n is genes of parent individuals; V_n^U is the upper limit value of V_n; V_n^L is the lower limit value of V_n.

Then, structure activation operation will check the control layer whether activated or not. The corresponding parameters layer will be altered when the control layer gene activates.

After each operation, the newborn individuals will through the evaluation operation to exanimate which individual is better among offspring and parents. This paper selects M group data as NN training, K group data as testing in this process, and then calculating the root mean square error (M.S.E.) E_{rms} as evaluated value which shows as (5). The lower value indicates the more close to NN convergence value.

$$E_{rms} = \sqrt{\frac{\sum_P^M \sum_j^N (T_j^p - Y_j^p)^2}{M \times N}} \tag{5}$$

where T_j^p is the target output of the jth output unit from Pth example. Y_j^p is the synthesis output of the jth output unit from Pth example. M is the number of examples. N is the number of units in the output layer.

After evaluation, the individual at lower evaluation value will be reserved to next operation. In this paper, we also proposed elite mechanisms to preserve the better chromosome so that converge speed will be accelerated: (1) If no more superior fitness value appeared in ten generation, a self-tuning formula will appropriately amend the ratios of crossover (p_c), mutation (p_m), and structure activation (p_s) respectively, which shows as shows as (6)–(8); (2) If the fitness value no longer appears superior value, the whole searching progress will stop. Then, these four factors will be set in NN.

$$p_c = p_c + k_1 \cdot (p_{c\_\max} - p_c) \tag{6}$$

$$p_m = p_m + k_2 \cdot (p_{m\_\max} - p_m) \tag{7}$$

$$p_s = p_s + k_3 \cdot (p_{s\_\max} - p_s) \tag{8}$$

where $p_{c\_\max}$ is the maximum ratio of crossover, $p_{m\_\max}$ is the maximum ratio of mutation, $p_{s\_\max}$ is the maximum ratio of structure activation, and k_1, k_2, k_3 are constant.

4.2.2. INN weighting optimization

When using sGA method, the four control factors of INNs can be optimized to be the optimal INN parameters. Then, INNs is trained again by the above optimal INNs parameters. The weights are associated with the connections of every neuron in each INN. The INN weights adjust automatically in the training phase by minimizing the error between the output from the network and the desired output, shown in Fig. 15. Finally, sGAINNs' optimal weights can be obtained in this process.

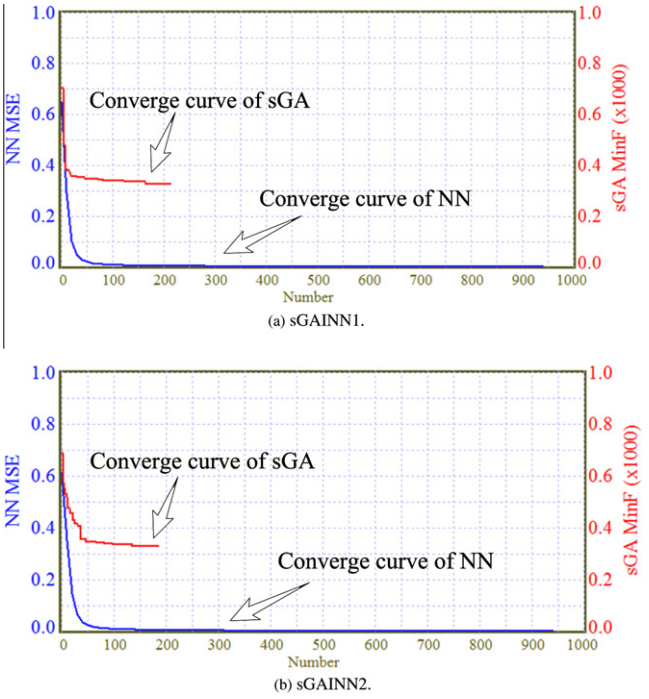

Fig. 15. The E_{rms} curve of sGAINN learning.

4.2.3. A synthesized reasoning engine

A comprehensive synthesized reasoning engine is proposed by this paper. The purpose of using comprehensive synthesized inference is to make the reasoning results of our purposed fault diagnosis matching experts' judgment. There are two inputs, which are estimated results of sGAINNs from full spectrum and half spectrum. The results inference of this diagnosis system to general faults such as unbalances, rotor bow, misalignment and fluid-induced instability was estimated by full spectrum, and result inference to particular faults from half spectrum such as whirl and whip. The comprehensive synthesized inference results in the experiment, shown in the later section, can obtain high identification ration in our proposed diagnosis system.

5. Experiment and results

The experimental setup depicts common faults including the unbalance, shaft bow, rub, misalignment, whip and whirl. The unbalance experiment setup used a normal rotor shaft with an unbalance disk in the rotor system. The bow experiment setup used a normal disk and a bow shaft. The rub experiment setup used two couples of copper bearing and a normal shaft. The misalignment experiment setup used two shafts and was connected with coupling. The fluid-induced instability experiment setup used fluid-induced bearing on the side of rotor.

In INNs, training data are gotten from full spectrum and half spectrum respectively. When sGA method is used to find optimal INN parameters, it need to exanimate the objective function, M.S.E. In our study, the minimum value indicated in Eq. (5) is expected. When the best INN parameters are found, the following INN will adopted as optimal INN parameters. The performance index of each INN learning is also evaluated by the root mean square error defined in Eq. (5). Fig. 15 shows the training results of unbalance which presents the two convergence curves of sGA and NN to the two INNs respectively.

After training phase, this paper proposed an examination method to ensure the faults identification probability for trained diagnosis system which relies on collecting other new faults samples. In this paper, an identification index is proposed to verify whether robust for our diagnosis system and to prevent "over-fitting" phenomenon occurs. This index is also called identification ratio which is defined as

$$R_i = \frac{P_{si}}{P_{others}} \tag{9}$$

where P_{si} is the identification possibility of assigned fault; P_{others} is the identification possibility of non-assigned faults, and Si corresponds to different faults.

Table 3 shows the examination results of "unbalance" which presents the identification ratios for five examination data. The possibility results of the unbalance after synthesized reasoning are shown in column 2 and 3. The results show that the possibility above 0.95 when rotor kit generates the unbalance fault. In contrast, the possibility is synthesized below 0.06 for the other faults which do not be generated from the rotor kit. In our study, the higher value indicated in Eq. (9) is expected. When the identification index in the examination stage is higher enough (In this paper, we define this ration is higher than 10.) that indicates the optimal parameters of INNs are found. Finally, our proposed diagnosis system will save these optimal parameters and weighting value of NNs. According the convergence figure, the best parameters of two INNs are shown as Table 4, respectively.

As mentioned above, six kinds of single fault are generated by the rotor kits and the vibration signals are fed into our proposed diagnosis system. The diagnosis result of single fault is shown in Table 5, where "$S1$: Unbalance", "$S2$: Bow", "$S3$: Misalignment", "$S4$: Rub", "$S5$: Whirl", "$S6$: Whip", "Normal: Normal state". Table 6 summarizes the identification ratio of single fault. The possibility results of the assigned fault after synthesized reasoning are shown

Table 3
The diagnosis result for unbalance.

Fault	Identification possibility		Identification ratio
$S1$	P_{s5}	P_{others}	R_1
Data 1	0.95	<0.050	19
Data 2	0.99	⩽0.050	19.8
Data 3	0.97	⩽0.060	16.17
Data 4	0.99	<0.060	16.5
Data 5	0.99	<0.060	16.5

Table 4
Optimal parameters of INNs.

INN parameters	INN 1 (full spectrum)	INN 2 (half spectrum)
Number of training times	899	961
Neuron numbers to hidden layer	16	12
Learning rate	0.988624	0.906182
Momentum factor	0.789144	0.774862

Table 5
The diagnosis result of single fault.

Single fault	Diagnosis value						
	$S1$	$S2$	$S3$	$S4$	$S5$	$S6$	Normal
$S1$	0.900	0.030	0.020	0.020	0.000	0.000	0.040
$S2$	0.000	1.000	0.000	0.000	0.000	0.000	0.000
$S3$	0.000	0.000	1.000	0.000	0.000	0.000	0.000
$S4$	0.000	0.000	0.020	1.000	0.000	0.000	0.000
$S5$	0.070	0.000	0.000	0.000	0.850	0.050	0.000
$S6$	0.000	0.000	0.000	0.000	0.053	0.840	0.000

Table 6
The identification ratio of single fault.

Fault	Identification possibility		Identification ratio
Si	P_{si}	P_{others}	R_i
***S*1**	0.900	<0.040	22.50
***S*2**	1.000	⩽0.000	∞
***S*3**	1.000	⩽0.000	∞
***S*4**	1.000	<0.020	50.00
***S*5**	0.85	<0.070	12.14
***S*6**	0.84	<0.053	15.84

Table 7
The diagnosis result of composite faults.

Composite fault		Diagnosis value						
Si	***Sj***	***S*1**	***S*2**	***S*3**	***S*4**	***S*5**	***S*6**	Normal
***S*2**	***S*3**	0.000	0.990	0.980	0.000	0.000	0.000	0.000
***S*3**	***S*6**	0.000	0.000	1.000	0.000	0.750	0.083	0.000

Table 8
The identification ratio of composite faults.

Faults		Identification possibility			Identification ratio	
Si	***Sj***	P_{si}	P_{sj}	P_{others}	R_i	R_j
***S*2**	***S*3**	0.990	0.980	⩽0.000	∞	∞
***S*3**	***S*6**	1.000	0.750	⩽0.083	12.05	9.03

in column 2 and 3. The results show that the possibility above 1.0 when rotor kit generates the assigned fault. In contrast, the possibility is synthesized below 0.07 for the other faults which don't be generated form the rotor kit.

In the experiment of composite faults, two faults are generated form the rotor kit and the vibration signals are fed into our proposed diagnosis system. Table 7 summarizes the diagnosis results where both ***Si*** and ***Sj*** are types of rotor fault. Table 8 summarizes the identification ratio of composite faults. P_{si} and P_{si} are both the identification possibility of assigned composite fault; P_{others} is the identification possibility of non-assigned faults. Both R_i and R_j are the identification ratios assigned composite fault. The possibility results of the assigned fault after synthesized reasoning are shown in column 3, 4 and 5. The results show that the possibility above 0.325 when rotor kit generates the assigned composite faults. In contrast, the possibility is synthesized below 0.09 for the other faults which don't be generated form the rotor kit.

6. Conclusions

This paper proposes a robust fault diagnosis system of rotating machine with the aim of avoiding unexpected failure that causes loss of production time and increases maintenance costs. This paper also proposed an adaptive fixed sample-rate order tracking method that is well-suited for high sweep rates and enhances signal analytic ability. The kernel of this diagnosis system includes a set of sGAINNs and synthesized reasoning engine. Six common faults of rotor system, unbalance, bow, misalignment, rub, whirl and whip, are generated from a rotor kit to verify the performance of this diagnosis system. The results showed that over 12.14 identification ratio are achieved for single fault and over 9.03 identification ratio are achieved for composite faults. We can apply the similar approaches on different faults to evaluate the identification ratio of our proposed approach. The advantage of this diagnosis system is that the trained epoch can be dramatically reduced, the over fitting problem can be avoided and the diagnosis accuracy can be improved.

Acknowledgement

The authors would like to thank Taiwan Power Research Institute for providing numerous helpful comments about common faults characteristics.

References

Bai, M. R., Jeng, J., & Chen, C. (2002). Adaptive order tracking technique using recursive least-square algorithm. *Transactions of the ASME, Journal of Vibrations and Acoustics, 124*, 502–511.

Donald, E. B., & Charles, T. H. (2003). *Fundamentals of rotating machinery diagnostics*. Amer. Society of Mechanical.

Diao, Y., & Passino, K. M. (2004). Fault diagnosis for a turbine engine. *Control Engineering Practice, 12*, 1151–1165.

Dasgupta, D., & McGregor, D. R. (1992). sGA: A structured genetic algorithm. Technical Report IKBS-8-92, University of Strathclyde.

Fu, L.-D., Chen, K.-S., Yu, J.-S., & Zeng, L.-C. (2006). The fault diagnosis for electro-hydraulic servo valve based on the improved genetic neural network algorithm. In *Proceedings of the 2006 international conference on machine learning and cybernetics* (pp. 2995–2999).

Fyfe, K. R., & Munck, E. D. S. (1997). Analysis of computed order tracking. *Mechanical of Systems and Signal Processing, 11*, 187–205.

Gebraeel, N., Lawley, M., Liu, R., & Parmeshwaran, V. (2004). Residual life predictions from vibration-based degradation signal: a neural network approach. *IEEE Transactions on industrial electronics, 51*(3), 694–700.

Goldman, P., & Muszynska, A. (1999). Application of full spectrum to rotating machinery diagnostics. *Orbit*, 17–21. First Quarter.

Hayashi, S., Asakura, T., & Zhang, S. (2002). Study of machine study of machine fault diagnosis System using neural networks. In *Proceedings of the international joint conference on neural networks* (Vol. 1, pp. 956–961).

Laws, B. (1998). When you use spectrum, don't use it halfway. *Orbit, 18*, 23–26.

Southwick, D. (1993). Using full spectrum plots. *Orbit, 14*, 19–21.

Southwick, D. (1994). Using full spectrum plots part2. *Orbit, 15*, 11–15.

Stephan, E., & Zhongxiao, P. (2008). Expert system development for vibration analysis in machine condition monitoring. *Expert System with Applications, 34*, 291–299.

Toutountzakis, T., Tan, C. K., & Mba, D. (2005). Application of acoustic emission to seeded gear fault detection. *NDT&E International, 38*, 27–36.

Wu, J.-D., & Liu, C.-H. (2009). An expert system for fault diagnosis in internal combustion engines using wavelet packet transform and neural network. *Expert System with Applications, 36*, 4278–4286.

Zhang, S., Asakura, T., Xu, X., & Xu, B. (2003). Fault diagnosis system for rotary machines based on fuzzy neural networks. *JSME International Journal, Series C: Mechanical Systems, Machine Elements and Manufacturing, 46*, 199–204.